Trap center study in hybrid organic-inorganic perovskite using thermally stimulated current (TSC) analysis

G. Gordillo, , C. A. Otálora, and , and M. A. Reinoso

Citation: Journal of Applied Physics **122**, 075304 (2017); doi: 10.1063/1.4999297
View online: http://dx.doi.org/10.1063/1.4999297
View Table of Contents: http://aip.scitation.org/toc/jap/122/7
Published by the American Institute of Physics

Trap center study in hybrid organic-inorganic perovskite using thermally stimulated current (TSC) analysis

G. Gordillo,[1,a)] C. A. Otálora,[2] and M. A. Reinoso[1,3]
[1]*Departamento de Física, Universidad Nacional de Colombia, 111321 Bogotá, Colombia*
[2]*Departamento de Química, Universidad Nacional de Colombia, 111321 Bogotá, Colombia*
[3]*Facultad de Ciencias de la Ingeniería, Universidad Estatal de Milagro, 091706 Milagro, Ecuador*

(Received 11 May 2017; accepted 5 August 2017; published online 18 August 2017)

This paper presents results of a study that allowed identifying states of traps in thin films of hybrid organic-inorganic perovskite compounds based on methylammonium lead halide with different compositions $CH_3NH_3PbX_3$ (X is Cl, Br or I) prepared by spin-coating, through Thermally Stimulated Current (TSC) measurements. Special emphasis was done in studying the influence of the composition and adsorption of oxygen on the depth of traps and on the density of states associated with trapping centers. Deconvolution of the TSC curves obtained from measurements made inside a vacuum chamber under different oxygen partial pressures, revealed the presence of traps centers whose activation energies are affected by the oxygen concentration. It was also found that TSC peaks do not appear in TSC measurements carried out at pressures less than 0.1 mbar, indicating that the possible nature of the identified traps centers is related to oxygen adsorbed superficially and/or located into the grain boundaries. [http://dx.doi.org/10.1063/1.4999297]

I. INTRODUCTION

Hybrid organic-inorganic perovskite materials as light absorbers are currently among the most promising candidates for thin film photovoltaic applications. Great advances in terms of efficiency have been achieved with this type of devices; however there is not enough information about their electrical transport properties and the relationship with the device efficiency. Recently, methylammonium lead halide ($MAPbX_3$; MA: CH_3NH_3, X: halogen) and its mixed-halide crystals, have been used as light harvesters for solar cells.[1–3] These devices are cost-effective due to their simple fabrication process and high power conversion efficiency (PCE), as a result, these cells have attracted a great deal of attention among researchers in the field. Perovskite solar cells have shown a rapid efficiency improvement (from 2.2% in 2006 to 22.1% in 2016),[4] achieving the highest efficiency of 21.1% at normal operating conditions.[5]

Recombination induced by defect states arising from chemical impurities and/or structural defects, has been identified as one of the hurdles for reaching high solar cell performances.[6] Defects may introduce trap and recombination centers, which have a direct influence on the transport phenomena of the charge carriers. Therefore, it is important to study the parameters characterizing such states. There are just a few experimental reports about defect characterization in hybrid organic-inorganic perovskite materials, however, thermally stimulated current (TSC) measurements are relatively easy to perform and provide detailed information on trap and/or recombination states.[7] TSC is known to be a very sensitive technique for studying point-defect and traps in semiconductors[8,9] which permits a rapid and straight forward survey of the gap states. Oxygen diffusion and iodide defects have been reported elsewhere[10] as a possible cause of photo-induced degradation of $MAPbI_3$ films. *Ab initio* simulations revealed that iodide vacancies are mainly responsible for this degradation.

The paper is organized as follows. Experimental and theoretical details of the study of trap centers in $CH_3NH_3PbX_3$ (X: I, Cl, Br) films, performed through TSC analysis are reviewed in Sec. II. Results regarding trap centers identified in thin films of organic-inorganic lead halide perovskites with different compositions ($MAPbI_3$, $MAPbI_2Br$, and $MAPbI_2Cl$) deposited in one step by spin-coating, as well as the activation energy and density of states associated to the traps are reported in Sec. III; followed by Conclusions in Sec. IV.

II. EXPERIMENTAL AND THEORETICAL DETAILS

A. Experimental

We studied $MAPbI_3$, $MAPbI_2Br$, and $MAPbI_2Cl$ films deposited on glass slides by spin-coating at 3000 rpm, from a solution 0.4M of the respective precursors in dimethyl sulfoxide (DMSO). The solution used for the synthesis of $MAPbI_3$ was prepared by mixing lead iodide (PbI_2) with methylammonium iodide (MAI) in equimolar proportions, while the synthesis of $MAPbI_2Br$ and of $MAPbI_2Cl$ was done mixing PbI_2 with methylammonium bromide (MABr) and methylammonium chloride (MACl) in equimolar proportions, respectively. The PbI_2 used was a commercial reagent (Sigma Aldrich) while the methylamine precursors were synthesized in our laboratory following the procedure described below: (i) the MAI was synthesized mixing 5 mL (0.051 mol) of hydroiodic acid (HI) to 67% with 15 mL of

a)Electronic mail: ggordillog@unal.edu.co

methylamine 2M in methanol and adding 20 mL of water at a controlled temperature of 273 K during 2 h. The MAI obtained (yellow color) was purified by repetitive rinsing in diethyl ether till pure MAI was obtained (white color) which was then dried at 373 K for 12 h; (ii) the MABr was synthesized mixing 10 mL (0.075 mol) of hydrobromic acid (HBr) to 45% with 25 mL of methylamine 2M in methanol and adding 20 mL of water at a controlled temperature of 273 K during 2 h. The MABr obtained (yellow color) was purified (white color) and dried following the same procedure used with MAI; and (iii) the MACl was synthesized mixing 3.7 mL (0.0447 mol) of hydrochloric acid (HCl) to 37% with 25 mL of methylamine 2M in methanol and adding 20 mL of water at a controlled temperature of 273 K during 2 h. The MACl obtained was purified and dried following the same procedure used with MAI and MABr.

For TSC measurements, electrical contacts of silver were deposited on the sample surface by evaporation, with 1 cm distance between them. The films were mounted on a Cu-plate placed inside a vacuum chamber, whose temperature can be varied (between 100 and 600 K) in a controlled way by means of an algorithm of control PID-PWM implemented using a virtual instrument (VI) developed with the software LabVIEW. The temperature was monitored by a NiCr-Ni thermocouple connected to an USB-600-NI hardware. This system includes facilities to generate ramps of temperature varying at a constant rate in the range of 2–20 K/min. The system developed to perform TSC measurements, allows estimating density of traps states with a lower limit of detection and quantification of approximately 6×10^{14} cm^{-3} and 2×10^{15} cm^{-3}, respectively.

The TSC measurements were done using the system whose block diagram is shown in Fig. 1 and following the next procedure: Initially the chamber is evacuated up to reaching a pressure of 10^{-2} mbar, and then oxygen is introduced continuously until reaching pressures in the range of 2 to 20 mbar; subsequently the sample is cooled at 180 K and

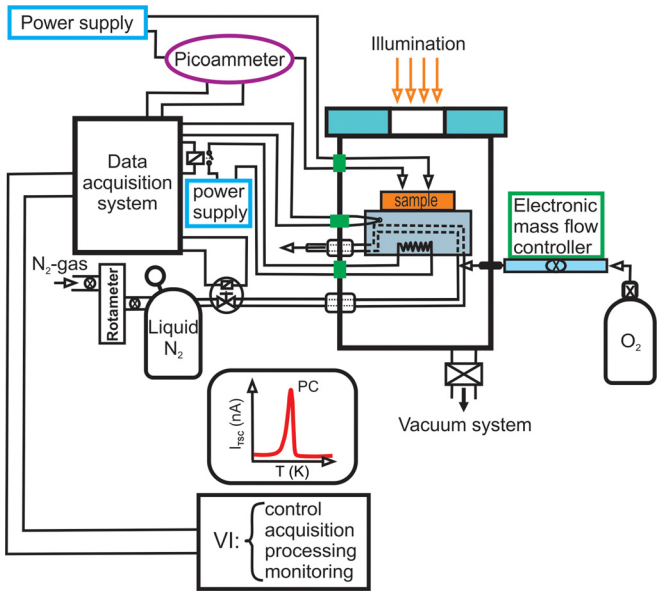

FIG. 1. Block diagram of the system implemented for the TSC measurements.

then illuminated during 15 min with an intensity of 500 W/m^2 using a 250 W halogen lamp. After that, the temperature is raised at a constant heating rate of 3 K/min until 300 K, keeping the DC voltage of 110 V and the oxygen pressure constant (both the bias voltage and oxygen flow are introduced as soon the sample temperature is stabilized at 180 K). The TSC system has facilities to register and acquire a datum in time intervals of one second and the reproducibility of the TSC spectra were verified through measurements realized to different samples prepared under the same conditions.

Before starting the evaluation of the samples through TSC measurements, a study was realized to find the parameters that give place to the best TSC response. In particular, the heating rate was varied between 2 and 6 K/min, and the bias voltage between 100 and 150 V_{DC}. TSC measurements carried out under different voltages of polarization indicated that normalizing the results in relation to the applied voltage, did not give rise to significant differences. In relation to the heating rate, it was found that the best TSC response is obtained under a heating rate of 3 K/min; this value was kept constant during the process of measurement, taking into account that the method of initial rise requires working with a constant heating ramp. Variation in the distance between electrodes may not be performed on the used measuring system.

Measurements realized to perovskite samples illuminated during periods of time greater than 15 min did not reveal significant changes neither in the form of the TSC curves nor in the temperature at which the peak appears; this behavior allowed us to assume that the studied perovskites do not degrade significantly under lighting effects. On the other hand, to reduce the effect of degradation induced by prolonged exposure in the atmosphere of oxygen, the measures were carried out by exposing the sample only during the 40 min that lasts the process; in addition the measures at different O_2-pressures were performed with freshly prepared samples.

B. Theoretical considerations

The thermally stimulated current (TSC) technique is a method frequently used to identify the presence of trap states in solids; it consists of filling centers after cooling down the material to low temperature and then heating the sample at a constant rate, showing the thermally stimulated current as the centers are emptied. The energy level within the band gap of a particular center is related to the temperature at which it is emptied, while the number of centers contributing to the observed current peak depends on the amount of stored charges which are released. The thermally stimulated current, due to a single center with an activation energy E_t, under slow re-trapping conditions is described by the equation[11]

$$I = I_0 \exp\left[-\frac{E_a}{kT} - \frac{v}{b}\int_{T_0}^{T} e^{-\frac{E_a}{kT}} dT\right], \quad (1)$$

where T_0 is the temperature at which heating begins after filling the center, k is the Boltzmann constant, and b is the

heating rate. The pre-exponential factor I_0 is a weak function of temperature and I exhibits a maximum as a function of temperature. As the temperature increases, the trapped charge carriers are released and this gives rise to current peaks. Consequently, a plot of current *versus* temperature is called the TSC spectrum. If more than one type of center is present, curves obtained from TSC studies may be expected to show several maxima depending upon the activation energy of the centers. In Eq. (1), v is the attempt-to-escape frequency, which is determined by the following expression:[12]

$$v = N_V v_{th} S, \tag{2}$$

where N_V is the effective density of states in the valence band, v_{th} is the thermal velocity of a charge carrier, and S is the capture cross section of the trap or recombination center.

The activation energy can be determined using the initial rise method which is valid for all types of recombination kinetics and is based on the assumption that when centers begin to empty as the temperature is increased, the TSC signal is proportional to $e^{-(E_a/kT)}$.[13] Therefore, this approach assumes that current is dominated by the first exponential factor in Eq. (1). Thus, a semi-logarithmic plot of the thermal stimulated current *versus* $1/kT$ gives a straight line with a slope value of $(-E_a)$.

The center concentration can be obtained taking into account the lower limit of the center density N_t, which can be found by integrating the TSC spectrum over time for each peak according to the following expression:[14]

$$\int_{T_0}^{T} I_{TSC} dT = b \int_{t_0}^{t_{final}} I dt = bQ = bqN_t V, \tag{3}$$

where Q is the quantity of charge released during a TSC experiment, which can be calculated from the area under the TSC peak, q corresponds to the electron charge, and V is the volume of the sample, which is calculated by multiplying the area of the cross section of the sample by the distance between electrodes. Several methods have been reported in the literature to evaluate center activation energy from the experimental TSC curves.[15–17] To analyze our results, we have chosen the initial rise method described above. Therefore, from the Arrhenius plots, corresponding to the initial rise of the TSC, the activation energies are found for the observed centers. This method was analyzed by Haake[18] demonstrating that up to a certain critical temperature value corresponding to about 40% of the TSC peak height, this assumption remains valid.

III. RESULTS

A. Sample characterization

Samples of $MAPbI_3$, $MAPbI_2Br$, and $MAPbI_2Cl$ were characterized through X-ray diffraction (XRD), scanning electron microscopy (SEM), and absorption coefficient measurements to determine the effect of substituting iodine by chlorine and by bromine in $MAPbI_3$ samples on the phase and crystalline structure as well as on the morphology and energy band gap. Typical XRD spectra are shown in Fig. 2.

A fitting of the experimental XRD spectra with XRD spectra calculated theoretically with the help of the program PowderCell, allowed us to establish that the $MAPbI_3$ films grow with a tetragonal structure and those of $MAPbI_2Br$ with a cubic structure, while the films of $MAPbI_2Cl$ grow basically with a mixture of a cubic and tetragonal perovskite structure; however some residual lead iodide is also present.

We investigated the morphological features of the perovskite film by means of SEM, as shown in Fig. 3. The SEM image of the $MAPbI_3$ film shows a larger surface coverage compared to the $MAPbI_2Br$ and $MAPbI_2Cl$ samples, with the grain domains of the $MAPbI_2Cl$ film being much smaller, whereas, large and more defined crystal grain domains are observed in $MAPbI_3$ and $MAPbI_2Br$ samples.

The band gap of the $MAPbI_3$, $MAPbI_2Br$, and $MAPbI_2Cl$ films was determined from absorption coefficient α, calculated from measurements of the diffuse reflectance (details in Ref. 19). For crystalline solids with an direct band gap, the dependence of the absorption coefficient α on the frequency ν can be approximated as $(\alpha h\nu)^2 = A\,(h\nu - E_g)$; therefore E_g can be obtained by extrapolating to zero a linear fit to a plot of $(\alpha h\nu)^2$ against $h\nu$. In Fig. 4 are displayed curves of α *vs.* $h\nu$ and $(\alpha h\nu)^2$ *vs.* $h\nu$ obtained for thin films of $MAPbI_3$, $MAPbI_2Br$, and $MAPbI_2Cl$. These results show that the $MAPbI_3$, $MAPbI_2Br$, and $MAPbI_2Cl$ films have energy band gap values of 1.55, 1.59, and 1.79 eV, respectively, which agree with those reported by other authors.[20,21]

B. TSC analysis

Figure 5 shows typical experimental TSC curves of thin films of $MAPbI_3$, $MAPbI_2Br$, and $MAPbI_2Cl$, obtained using the initial rise method from measurements carried out on samples kept under an oxygen partial pressure inside the measuring chamber of 2 and 20 mbar, respectively. This result shows that varying the temperature between 220 and

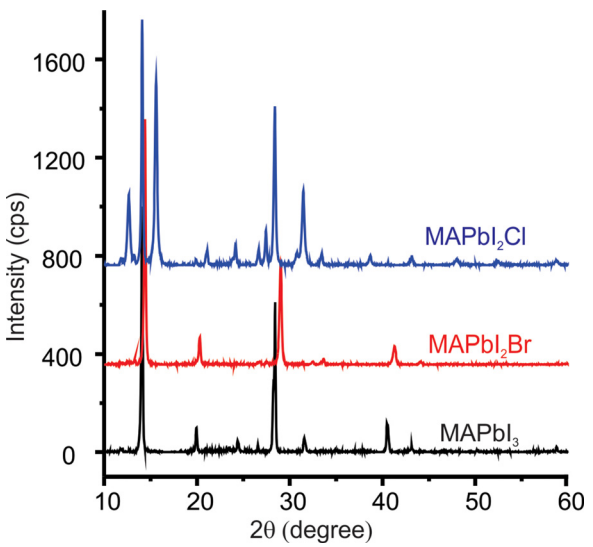

FIG. 2. XRD spectra of thin films of $MAPbI_3$, $MAPbI_2Br$, and $MAPbI_2Cl$.

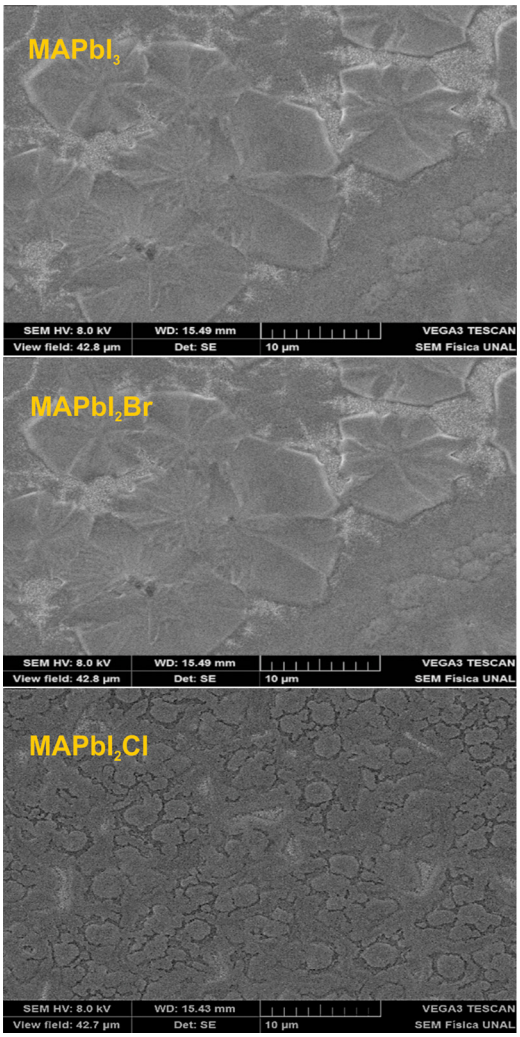

FIG. 3. SEM images of thin films of $MAPbI_3$, $MAPbI_2Br$, and $MAPbI_2Cl$.

300 K, at a rate of 3 K/min, only one TSC peak is observed between 250 and 260 K.

It is observed from Fig. 5, that the intensity of the TSC curves obtained from measurements performed at a pressure of 20 mbar is significantly higher than that of the sample exposed at a pressure of 2 mbar, indicating that the density of trapped charge carriers increases when the pressure inside the measuring chamber is increased. This behavior may be attributed to the capture of electrons in trap states coming from oxygen molecules chemisorbed on $MAPbI_3$ [$O_{2(g)} + e^- \rightarrow O_2^-{}_{(ad)}$]; subsequent releasing of trapped electrons from the sample exposed to a higher density of oxygen molecules gives rise to higher current peaks. Measurements carried out on samples under pressures of less than 0.1 mbar do not present TSC peaks confirming that the behavior of the TSC curves observed in Fig. 2 is mainly attributed to effects of adsorption of oxygen. The non-presence of TSC peaks at pressures lower than 0.1 mbar could also be due to the fact that under these conditions the density of trap states is less than the lower limit of detection of the measurement system (6×10^{14} cm^{-3}). The results also reveal that the $MAPbI_2Cl$ samples have no detectable sub-gap trap states at pressures lower than 0.1 mbar, indicating that the substitution of Cl by I in $MAPbI_3$ films, strongly reduces the density of trap states in the absence of oxygen, to values below 10^{14} cm^{-3} which is the lower detection limit of our measurement system. This fact also can be related with the presence of PbI_2 acting as a possible trap state passivating; this affirmation is supported by time-resolved photolumiunescence studies carried out on PbI_2-rich perovskite films by other authors,[22] which revealed a longer lifetime due to suppressed defect trapping states, compared to the PbI_2-poor samples, suggesting that PbI_2 can locally passivate the defect states of the perovskite film. Similar results have been reported in previous publications.[23–25] These results are important for further improvement of the solar cells based on perovskite with excess of PbI_2.

In addition, from a first sight, the characteristics of a peak quite wide and asymmetric, indicate the presence of other overlapped peaks. In an attempt to analyze this behavior, we deconvoluted the TSC-curves into several peaks. Considering that the slope at the beginning of the rise TSC curve and at the end of its decay is very pronounced

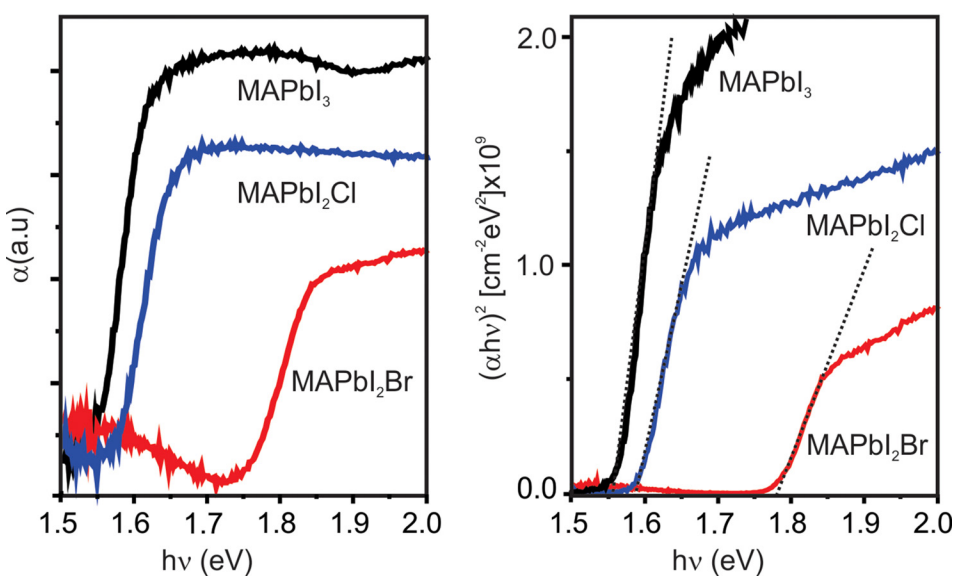

FIG. 4. Curves of α *vs.* $h\nu$ and $(\alpha h\nu)^2$ *vs.* $h\nu$ corresponding to thin films of $MAPbI_3$, $MAPbI_2Br$, and $MAPbI_2Cl$.

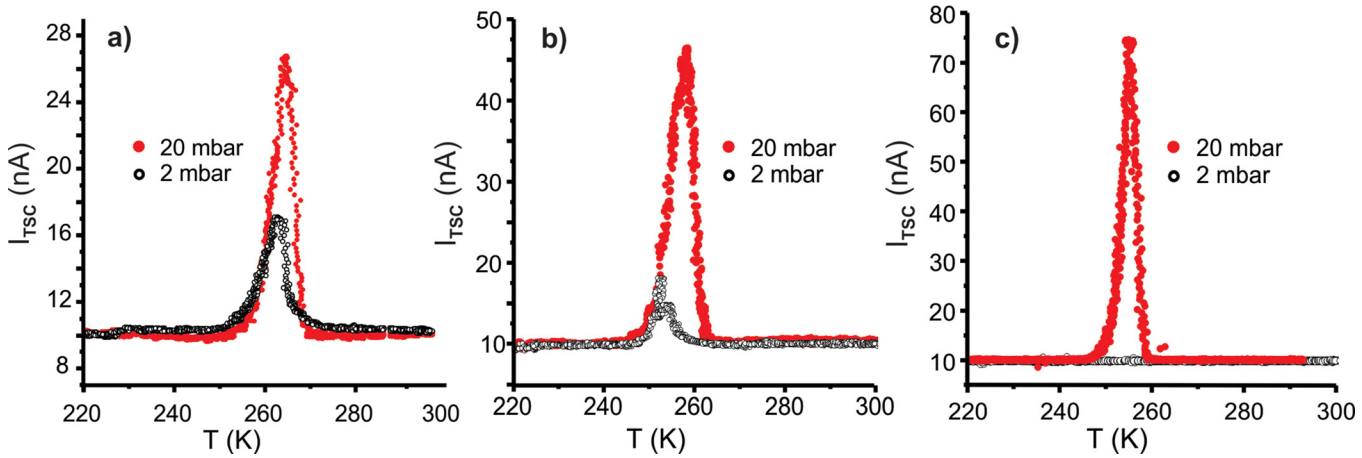

FIG. 5. TSC curves of thin films of (a) $MAPbI_3$, (b) $MAPbI_2Br$, and (c) $MAPbI_2Cl$, obtained from measurements performed under oxygen partial pressures of 2 and 20 mbar, respectively.

(behavior that is characteristic of a Gaussian distribution), we believe that it is more appropriate to realize the fitting with Gaussian functions instead of Lorentzians, that present much smaller slopes.

In this work, the deconvolution of the TSC peaks was done without fixing *a priori* the end position and the width of the Gaussian functions; however as starting data of the iteration process, both the number of peaks as their respective initial positions as well as the tolerance were provided. Subsequently the program (Origin 8.0) found the position, width, and intensity of the Gaussian curves that give rise to the best fit to the experimental spectra.

In order to find the best fitting to the experimental TSC curves, we deconvoluted the TSC curves based on Gaussians functions into one, two or three peaks; by example, for a typical $MAPbI_3$ film under a pressure of 20 mbar (see Fig. 6) we found that, the best fit is obtained deconvoluting the experimental TSC curves into three peaks, the result of which was confirmed using as a figure of merit the value of the reduced chi-square. Reduced chi-square values of 0.317, 0.178, and 0.144 were found for curve fitting with one, two, and three peaks, respectively.

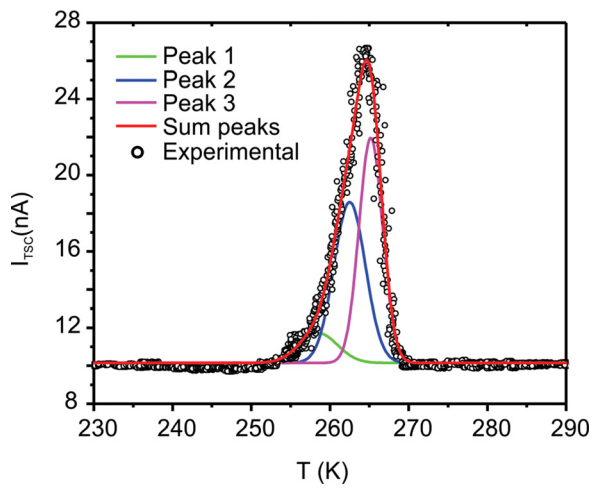

FIG. 6. Deconvolution of the TSC curve obtained from measurements carried out on a $MAPbI_3$ film under a pressure of 20 mbar. The red line is the sum of three peaks used to deconvolute the experimental TSC curve.

In the deconvolution approach, the sum of three peaks matches the experimental TSC curve, indicating that the $MAPbI_3$ film exposed to a partial pressure of 20 mbar presents trap or recombination centers with three different activation energies [see Fig. 7(a)]. It was also found that in the first deconvolution approach of the TSC curve of $MAPbI_3$ films exposed to a partial pressure of 2mbar, the sum of two peaks matches the experimental data, indicating that in this case the $MAPbI_3$ sample presents trap or recombination centers with two different activation energies. The fitting with Gaussian curves of the experimental TSC curve of the $MAPbI_2Br$ sample indicated that the $MAPbI_2Br$ film exposed to a partial pressure of 20 mbar also present trap centers with three different activation energies [see Fig. 7(b)], whereas the $MAPbI_2Br$ film exposed to a partial pressure of 2 mbar presents trap centers with just two different activation energies. The analysis of the experimental TSC curve obtained for the $MAPbI_2Cl$ sample from measurements carried out at 20 mbar indicated that these type of samples present just one activation energy [see Fig. 7(c)]; on the contrary, measurements realized to $MAPbI_2Cl$ films under a partial pressures of 2 mbar do not exhibit TSC peaks.

Using the initial rise method, the activation energies of the $MAPbI_3$, $MAPbI_2Br$, and $MAPbI_2Cl$ samples were determined; for that, a semi-logarithmic plot of the current *versus* 1/kT gives a straight line with a slope value of $(-E_a)$. Figure 7 shows the activation energy values of thin films of $MAPbI_3$, $MAPbI_2Br$, and $MAPbI_2Cl$ exposed to oxygen partial pressures of 2 and 20 mbar, which were obtained from the respective Arrhenius plot.

TSC measurements allow determining not only the activation energies of the trap states but also their density, which were calculated from the deconvoluted TSC spectra *versus* time, by using Eq. (3) where the sample volume was calculated as described above (Sec. II B). In Table I are listed values of activation energy and density of states N_t associated with the traps identified in $MAPbI_3$, $MAPbI_2Br$, and $MAPbI_2Cl$ films exposed to oxygen partial pressures of 2 and 20 mbar, respectively.

Due to the complexity of the samples studied, it is quite difficult to determine the nature of the centers found; however,

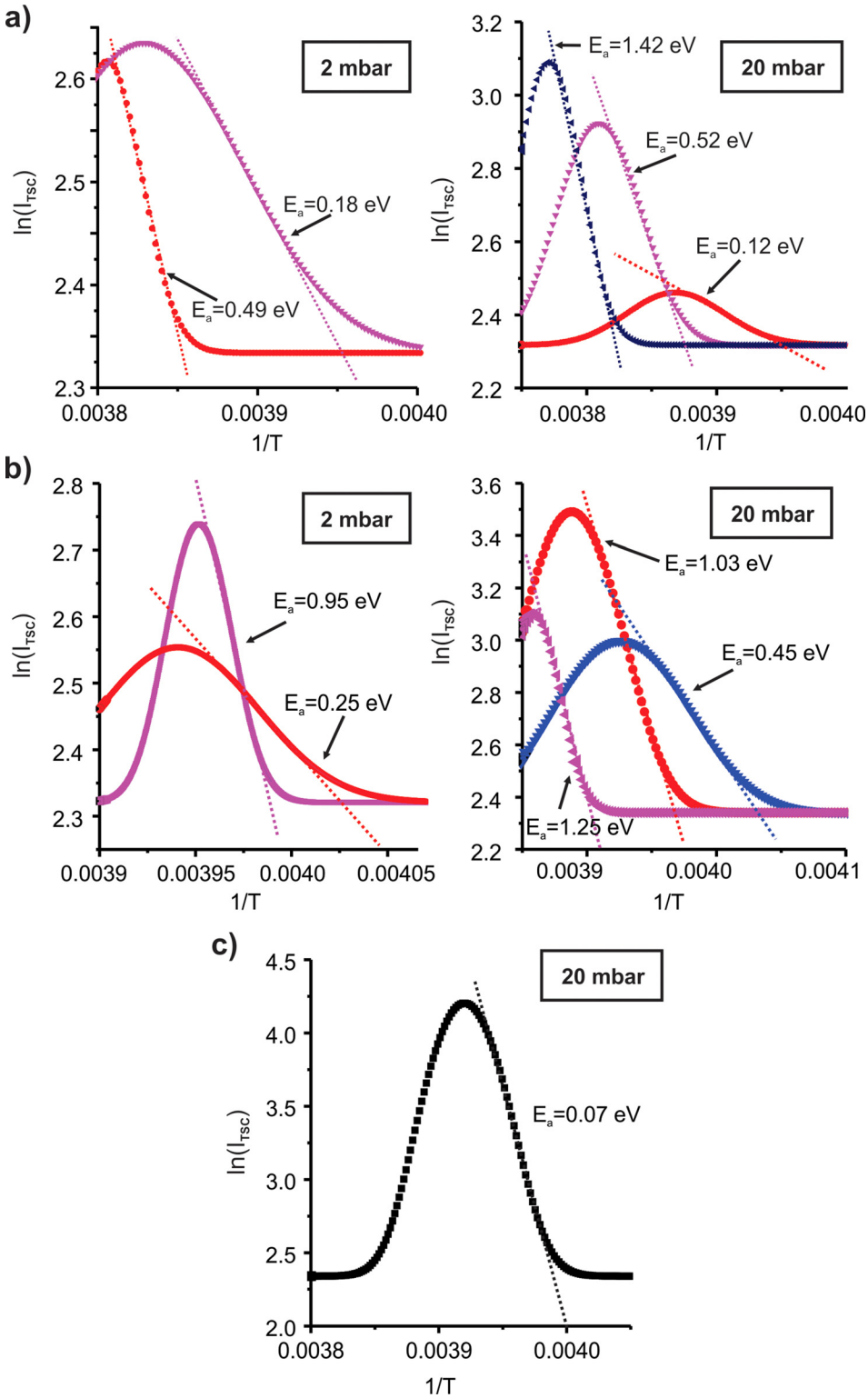

FIG. 7. Arrhenius plot showing the activation energy values of (a) $MAPbI_3$, (b) $MAPbI_2Br$, and (c) $MAPbI_2Cl$ films exposed to an oxygen partial pressure of 2 mbar and 20 mbar, respectively.

we think that the observed states of some energy levels can be associated with oxygen adsorbed at the surface of the sample and/or located in the crystalline grains boundaries. The shallow levels located at 0.12 eV, 0.18 eV (in $MAPbI_3$ samples), 0.25 eV (in $MAPbI_2Br$ films), and 0.07 eV (in $MAPbI_2Cl$ films) can be considered as traps; whereas the deep levels at 0.48 eV, 0.52 eV and 1.42 eV (in $MAPbI_3$ samples), 0.45 eV, 0.95 eV, and 1.03 eV and 1.25 eV (in $MAPbI_2Br$ films) can be considered as trap assisted recombination centers.

Similar values of E_a were found for $MAPbI_3$ films through transient photoconductivity measurements carried out at different temperatures and theoretical simulation of the relaxation curves; details of this study is given in Ref. 26. Using values of the time constants τ obtained from the theoretical simulation of the curves of photocurrent decay measured at temperatures ranging from 25 to 65 °C, the activation energy E_a of states corresponding to three different traps was estimated from the slope of the Arrhenius plots

TABLE I. Values of activation energy E_a and density of states N_t associated with traps, estimated for $MAPbI_3$, $MAPbI_2Br$, and $MAPbI_2Cl$ thin films exposed to an oxygen partial pressure of 2 and 20 mbar.

		2 mbar		20 mbar	
		N_t (cm^{-3})	Ea (eV)	N_t (cm^{-3})	Ea (eV)
$MAPbI_3$	Trap 1	9.14×10^{16}	0.18	2.16×10^{16}	0.12
	Trap 2	4.75×10^{16}	0.49	7.29×10^{16}	0.52
	Trap 3	…	…	7.59×10^{16}	1.42
$MAPbI_2Br$	Trap 1	2.82×10^{16}	0.25	1.52×10^{17}	0.45
	Trap 2	2.30×10^{16}	0.95	2.21×10^{17}	1.03
	Trap 3	…	…	9.01×10^{16}	1.25
$MAPbI_2Cl$	Trap 1	…	…	4.11×10^{17}	0.07

$\left[\tau = \tau_0 e^{-(E_a/kT)}\right]$. It was found that, in general, the photocurrent response is affected by both trap assisted fast recombination processes and traps whose activation process is delayed, being the contribution in the intensity of the photocurrent of the first process greater that the second one. Evidence was found that the $MAPbI_3$ film exhibits a deep trap state at around 459 meV attributed to trap assisted recombination; furthermore, the $MAPbI_3$ films present shallow trap states at 129 and 24 meV that correspond to states of traps whose activation process is delayed.

The presence of deep trap states at around 508 meV was also found in $MAPbI_3$ films from thermally stimulated current (TSC) measurements.[27] Defect states (at 0.16 eV above the valence band) have been identified in $MAPbI_3$ films using admittance spectroscopy.[28] According to density functional calculations,[29] this defect energy could potentially be ascribed to iodine interstitials.

The results presented in Table I reveal that the density of states N_t associated with the different traps increase by increasing the oxygen partial pressure inside the measurement chamber. The values of N_t estimated for the traps identified in the three studied compounds are in general quite high ($>10^{16}\,cm^{-3}$), and similar results have been reported by other authors using different techniques;[30,31] however the compounds $MAPbI_2Br$ and $MAPbI_2Cl$ are characterized by having densities of trap states significantly higher than those of the $MAPbI_3$ films. These results indicate that the observed degradation in hybrid organic-inorganic compounds, when these are exposed to the environment, could be related to the generation of high densities of traps states, induced by adsorption of oxygen.

IV. CONCLUSIONS

The thermally stimulated current technique has been used to identify the presence of trap centers in thin films of organic-inorganic lead halide perovskites with different compositions ($MAPbI_3$, $MAPbI_2Br$, and $MAPbI_2Cl$) prepared by spin-coating, as well as to calculate both the activation energy and density of states associated with the traps. It was found that oxygen adsorbed at the surface of the sample and/or located into the grain boundaries, significantly affects the traps and recombination processes; the TSC study revealed that the $MAPbI_3$ and $MAPbI_2Br$ films exposed to oxygen, present traps or recombination centers characterized by having both shallow levels which could be classified as trap and deep levels which could be classified as trap assisted recombination centers. On the other hand, it was proved that the $MAPbI_2Cl$ films have only one shallow trap level, indicating that recombination *via* traps processes predominates in this type of compounds.

The density of trap states N_t, estimated by integrating the TSC spectrum over time for each peak, indicated that the N_t value increases by increasing the oxygen partial pressure inside the measurement chamber. It was found that the density of states associated with the traps identified in the three studied compounds is in general quite high ($>10^{16}\,cm^{-3}$), with the N_t value of the traps identified in the $MAPbI_2Br$ and $MAPbI_2Cl$ films being significantly higher than that of the $MAPbI_3$ films. These results indicate that the observed degradation in organic-inorganic lead halide perovskites, when these are exposed to the environment, could be related to the generation of high densities of trap states, induced by adsorption of oxygen.

ACKNOWLEDGMENTS

This work was supported by the Colciencias (Contract No. 184/2016) and the Universidad Nacional de Colombia, Sede Bogotá, Facultad de Ciencias, Grupo GMS&ES, Bogotá DC, Colombia (Proy. 20287 supported by DIB).

[1]M. M. Lee, J. Teuscher, T. Miyasaka, T. N. Murakami, and H. J. Snaith, Science **338**, 643 (2012).
[2]H. S. Kim, C. R. Lee, J. H. Im, K. B. Lee, T. Moehl, A. Marchioro, S. J. Moon, R. Humphry-Baker, J. H. Yum, J. E. Moser, M. Gratzel, and N. G. Park, Sci. Rep. **2**, 591:1–7 (2012).
[3]J. H. Noh, S. H. Im, J. H. Heo, T. H. Mandal, and S. I. Seok, Nano Lett. **13**, 1764 (2013).
[4]S. Hoefler, G. Trimmel, and T. Rath, Monatsh. Chem. **148**(5), 795 (2017).
[5]M. Saliba, T. Matsui, J. Y. Seo, K. Domanski, J. P. Correa-Baena, M. Khaja, S. M. Zakeeruddin, W. Tress, A. Abate, A. Hagfeldtd, and M. Grätzel, Energy Environ. Sci. **9**, 1989 (2016).
[6]S. Siebentritt, Thin Solid Films **535**, 1 (2013).
[7]M. Courel, O. Vigil-Galán, D. Jiménez-Olarte, M. Espíndola-Rodríguez, and E. Saucedo, J. Appl. Phys. **116**, 134503 (2014).
[8]E. Turan, M. Zor, A. S. Aybek, and M. Kul, Phys. B: Phys. Condens. Matter **395**, 57 (2007).
[9]N. S. Yuksek, N. M. Gasanly, and H. Ozkan, Semicond. Sci. Technol. **18**, 834 (2003).
[10]N. Aristidou, C. Eames, I. Sanchez-Molina, X. Bu, J. Kosco, M. S. Islam, and S. A. Haque, Nat. Commun. **8**, 15218 (2017).
[11]N. S. Mohan and R. Chen, J. Phys. D: Appl. Phys. **3**, 243 (1970).
[12]N. M. Gasanly and T. Yildirim, Acta Phys. Pol. A **119**, 437 (2011).
[13]R. Chen and S. W. Mckeever, *Theory of Thermoluminescence and Related Phenomena* (Word Scientific, Singapore, 1997), p. 100.
[14]J. Schafferhans, A. Baumann, C. Deibel, and V. Dyakonov, Appl. Phys. Lett. **93**, 093303 (2008).
[15]J. M. Wrobel, A. Gubanski, E. Płaczek-Popko, J. Rezmer, and P. Becla, J. Appl. Phys. **103**, 063720 (2008).
[16]G. Micocci and A. Tepore, J. Appl. Phys. **80**, 894 (1996).
[17]T. Yıldırım and N. M. Gasanly, Solid State Sci. **11**, 1562 (2009).
[18]C. H. Haake, J. Opt. Soc. Am. **47**, 649 (1957).
[19]A. B. Murphy, Appl. Opt. **46**, 3133 (2007).
[20]Y. Chen, T. Chen, and L. Dai, Adv. Mater. **27**, 1053 (2015).
[21]Y. Zhao and K. Zhu, J. Am. Chem. Soc. **136**(35), 12241 (2014).
[22]S. Chen, X. Wen, J. S. Yun, S. Huang, M. Green, N. J. Jeon, W. S. Yang, J. H. Noh, J. Seo, S. I. Seok, and A. Ho-Baillie, ACS Appl. Mater. Interfaces **9**, 6072 (2017).
[23]Q. Chen, H. Zhou, T. B. Song, S. Luo, Z. Hong, H. S. Duan, L. Dou, Y. Liu, and Y. Yang, Nano Lett. **14**(7), 4158 (2014).

[24]Y. C. Kim, N. J. Jeon, J. H. Noh, W. S. Yang, J. Seo, J. S. Yun, A. Ho-Baillie, S. Huang, M. A. Green, J. Seidel, T. K. Ahn, and S. I. Seok, Adv. Energy Mater. **6**(4), 1502104 (2016).
[25]T. J. Jacobsson, J. P. Correa-Baena, E. H. Anaraki, B. Philippe, S. D. Stranks, M. E. F. Bouduban, W. Tress, K. Schenk, J. Teuscher, J. E. Moser, H. Rensmo, and A. Hagfeldt, J. Am. Chem. Soc. **138**, 10331 (2016).
[26]G. Gordillo, C. A. Otálora, and A. A. Ramirez, Phys. Chem. Chem. Phys. **18**, 32862 (2016).
[27]A. Baumann, S. Väth, P. Rieder, M. C. Heiber, K. Tvingstedt, and V. Dyakonov, J. Phys. Chem. Lett. **6**(12), 2350 (2015).
[28]H. S. Duan, H. Zhou, Q. Chen, P. Sun, L. Song, T. B. Song, B. Bob, and Y. Yang, Phys. Chem. Chem. Phys. **17**, 112 (2015).
[29]M. H. Du, J. Mater. Chem. A **2**, 9091 (2014).
[30]S. D. Stranks, V. M. Burlakov, T. Leijtens, J. M. Ball, A. Goriely, and H. J. Snaith, Phys. Rev. Appl. **2**, 034007 (2014).
[31]G. Xing, N. Mathews, S. S. Lim, N. Yantara, X. Liu, D. Sabba, M. Grätzel, S. Mhaisalkar, and T. C. Sum, Nat. Mater. **13**, 476 (2014).